

# Cyclodextrin-grafted redox-responsive hydrogel mediated by disulfide bridges for regulated drug delivery

Xin Xu<sup>a</sup>, Jinku Xu<sup>a</sup>, Zeyuan Sun<sup>a,b</sup> and Derkach Tetiana<sup>b</sup>

<sup>a</sup>School of Chemistry and Chemical Engineering, Qilu University of Technology (Shandong Academy of Sciences), Jinan, China; <sup>b</sup>College of Pharmacy, Kyiv National University of Technologies and Design, Kyiv, Ukraine

## ABSTRACT

In this paper, a novel mono-methacrylated  $\beta$ -cyclodextrin ( $\beta$ -CD) monomer mediated by disulfide bond was synthesized, and then thermal copolymerized with HEMA monomer in the presence of a little crosslinker to prepare redox-responsive hydrogel for regulated drug delivery. The structure of the monomer was confirmed by FTIR, <sup>1</sup>H NMR, <sup>13</sup>C NMR spectroscopy. The substitution degree of polymerizable methacrylated group grafted onto  $\beta$ -CD was about 1 by calculating by <sup>1</sup>H NMR (0.987) and element analysis (0.937). The mono-methacrylated  $\beta$ -CD monomer can well copolymerize with 2-hydroxyethyl methacrylate (HEMA) monomer with gel fraction over 80%. The hydrogel shows low cytotoxicity, and copolymerization of the mono-methacrylated  $\beta$ -CD monomer in the hydrogels increases its equilibrium swelling degree (ESD) and tensile strength, while its transmittance slightly decreases. Drug loading and release rate are dependent on the  $\beta$ -CD content. The hydrogel with high  $\beta$ -CD content of 13.83 wt% shows 1.8 and 8.5 folds puerarin (PUE) and curcumin (CUR) loading than pure pHEMA hydrogel, respectively. The incorporation of  $\beta$ -CD sustained drug release, especially CUR release was prolonged more than 24 h from 5 h of pure pHEMA hydrogel (80% release). The hydrogels are highly sensitive to reduced glutathione (GSH), and low concentration of GSH of 3 mM can significantly accelerate drug release rate. The higher of  $\beta$ -CD content, the more sensitive the hydrogels to GSH, resulting in rapider drug release rate.

## ARTICLE HISTORY

Received 30 January 2024  
Accepted 18 May 2024

## KEYWORDS



Cyclodextrin; redox-responsive hydrogel; disulfide bridges; curcumin; puerarin


## 1. Introduction

Hydrogels, a three-dimensional crosslinked polymer network with hydrophilic properties, have good bio-compatible, similar flexibility to human tissue, and have been considered as potential systems for the development of tissue-engineered scaffolds and drug delivery systems. For this hydrogel drug delivery system, two main approaches are used for drug loading: (a) physical encapsulating drug in the hydrogel [1–3], and (b) coupling drug molecule to the gel backbone through chemical bond [4–7]. The first method is more commonly used for drug loading. However, most of the gel matrix is hydrophilic matrix; hydrophobic drugs are not suitable for it; if the loading is carried out by physical methods, it will lead to low drug loading and may be associated with the phenomenon of burst release. The second approach is not considered as a universal method because it requires additional chemical modification of the drug. This may result in the loss of the active essential group and decrease the drug's therapeutic efficacy [8,9]. How

to increase the different hydrophobic drug content in hydrogels without modifying the drug structure one by one and control drug release are key problems in the development of long-term drug delivery systems.

At present, the method commonly used to improve the loading capacity of hydrogel is to introduce nanoparticles (e.g., liposomes [10], nanocapsules [11], etc.) that can encapsulate the drug or molecules (cyclodextrins) that can form complexes with the drug into hydrogels. Cyclodextrins are cyclic oligosaccharides consisting of 6, 7, and 8 glucose units ( $\alpha$ ,  $\beta$ , and  $\gamma$ -CD, respectively) bonded by 1–4 carbon bonds, which contain a hydrophobic cavity and a hydrophilic surface [12,13]. The existence of the hydrophobic cavity allows them to form complexes with hydrophobic molecules to address the problem of low water solubility of drugs. Among them,  $\beta$ -CD has been widely investigated for its good biocompatibility, strong encapsulation properties, and easy structural modification. To avoid burst release of the drug,  $\beta$ -CD is commonly incorporated into the gel

**CONTACT** Jinku Xu  [jkxu2003@126.com](mailto:jkxu2003@126.com)  School of Chemistry and Chemical Engineering, Qilu University of Technology (Shandong Academy of Sciences), Jinan 250353, China

 Supplemental data for this article can be accessed online at <https://doi.org/10.1080/15685551.2024.2358581>

© 2024 The Author(s). Published by Informa UK Limited, trading as Taylor & Francis Group.

This is an Open Access article distributed under the terms of the Creative Commons Attribution-NonCommercial License (<http://creativecommons.org/licenses/by-nc/4.0/>), which permits unrestricted non-commercial use, distribution, and reproduction in any medium, provided the original work is properly cited. The terms on which this article has been published allow the posting of the Accepted Manuscript in a repository by the author(s) or with their consent.

backbone through chemical bond [14–17] rather than physical loading at present [18,19]. However, it is unable to control drug release in this way; drug loading and release depend on the affinity of the drug between  $\beta$ -CD, and high inclusion constant helps to increase drug loading and delay drug release. However, high inclusion constant drugs may also cause some problems, such as incomplete release or long-term low-dose release, resulting in drug loss and even drug resistance issues. The ideal drug release rate of drug-loaded hydrogel should be as slow as possible during the initial drug release stage, and then be regulated to accelerate release after the burst release.

Currently, hydrogel systems are becoming more 'intelligent' by introduction of responsive polymers. Disulfide bond can be broken in high reducing glutathione environments that was highly expressed in cancer cells [20]. Therefore, disulfide bond has been widely introduced into the polymer structure of drug carriers. Trotta et al. developed a nanosponge that is bio-responsive to GSH external concentration triggering for rapid nanocarrier destabilization inside cells, leading to efficient intracellular drug release through disulfide-bond cleavage. Cyclodextrin dimers [21] or duplexes [22] have also been synthesized using one, two, and three disulfide linkages, respectively. Disulfide-mediated redox-responsive cyclodextrin-based nanoplateform has demonstrated the ability of tumor targeted drug delivery, in which the nanocarrier was usually formed by host-guest self-assembly. Qimin Jiang et al. [23] synthesized a reduction degradable and photosensitive disulfide-

containing azobenzene-terminated branched poly (2-(dimethylamino)ethyl methacrylate)s (Az-SS-BPDMs) by ATRP reaction of monomer and a crosslinker mediated by disulfide bridges. The polymer can form supramolecular host-guest self-assembly systems with poly(cyclodextrin) (PCD) for non-viral gene delivery vectors. However, host-guest self-assembly leads to hydrophobic cavities of cyclodextrins to be occupied, reducing the drug loading capacity by inclusion complex between cyclodextrin and drug molecules. There are some reports of disulfide cross-linked hydrogel and  $\beta$ -CD hydrogel as shown in Table 1.

Puerarin is a traditional Chinese medicine extracted from wild kudzu roots. Although puerarin is insoluble in water, it can be solubilized into liquid formulations, such as 1.0 wt% eye drops, which have been used in clinical treatment of glaucoma and high intraocular pressure and can maintain long-term intraocular hypotension. Curcumin is another active ingredient extracted from traditional Chinese medicine with lower water solubility. It has been widely exploited for its anti-inflammatory, antioxidant, anti-microbial, and anti-tumor effects [24,25], in addition to being used to treat corneal and retinal neovascularisation, and to inhibit the proliferation of lens epithelial cells and retinal pigment epithelium [26,27]. Both drugs can be used for ocular administration to treat eye diseases. However, its low water solubility and the biofilm barriers limit its application, and how to improve its water solubility and biological barrier membrane penetration is a major challenge for its application [28]. The poor bioavailability of current

**Table 1.** Disulfide cross-linked hydrogel and  $\beta$ -CD hydrogel for drug delivery.

Method of drug -load	Drug	Components	Disulfide bond source	Ref.
Drugs physically encapsulated in the disulfide cross-linked hydrogel	DOX	Low-generation peptide dendrimer-SS-low-generation peptide dendrimer	Dimethyl l-Cystinate Bis(acrylamide)	1
	BSA	Oxidized hyaluronic acid-SS-oxidized hyaluronic acid	3,3' -dithiobis (propionohydrazide)	2
	MTX	Disulfide-cross-linked hydrogel of methoxy poly(ethylene glycol)-poly(L-phenylalanine-co-L-cystine)	L-cystine	3
Drug molecules are coupled to the hydrogel backbone via disulfide bond	CPT	Poly(ethylenimine)-SS-CPT/oxidized sodium alginate-IR780	2,2' -dithiodiethanol	4
	OVA	Methacrylated dextran- trimethyl aminoethyl methacrylate-SS-OVA	Pyridyldisulfide-containing methacrylamide (thiol-disulfide exchange)	5
	RC7 peptide	RC7-SS- RC7	Cysteine amino acid (thiol-disulfide exchange)	6
	CTX PI103	PEG-tethered methacrylic acid-bis(ethylene methacrylate) disulfide-CTX/PI103	2,2' -dithiodiethanol	7
Drug complexes physically encapsulated in hydrogel	MTX	$\beta$ -CD/kappa-carrageenan		18
	GA	HP $\beta$ -CD/bacterial cellulose/poly (vinyl alcohol)		19
Drug complexes are coupled to the hydrogel backbone via chemical bond (undegradable)	NFX	Poly (ethylene glycol)- Hexamethylene diisocyanate- $\beta$ -CD		14
	IBU	Polyvinyl alcohol- $\beta$ -CD		15
	IBU-Na			
	CUR	Poly( $\beta$ -cyclodextrin triazine)		16
	PTX RST	$\beta$ -CD-polyvinylpyrrolidone-co-poly (2-acrylamide-2-methylpropane sulphonic acid)		17

conventional ophthalmic solutions and the clearing mechanisms at the corneal surface (including lacrimation, tear turnover, and tear dilution) can lead to drug loss; the increase of dosing frequency to maintain therapeutic concentration may also cause side effects and low patient adherence [29,30]. All these factors make the ocular application of puerarin and curcumin become more difficult. How to improve the drug content in a single dose, the bio-barrier membrane permeability and prolong the corneal residence time is the major challenge for the ophthalmic application. Cheng et al. [30] modified HPMC with mucosal adhesion properties to obtain methacrylic anhydride-modified hydroxypropyl methylcellulose hydrogel to prolong the drug residence time in the eye. However, there are some issues that have not been resolved, such as the low amount of drug available in a single dose and uncontrolled drug release. Both puerarin and curcumin can form inclusion with  $\beta$ -CD, and curcumin indicates a higher inclusion constant than puerarin [31].

Based on above problems of gel drug delivery system, a novel mono-methacrylated  $\beta$ -CD monomer mediated by disulfide bond was synthesized, and then copolymerized with HEMA monomer to prepare redox-responsive hydrogel. One side, grafted  $\beta$ -CD in the hydrogel can increase affinity of the gel backbone to drug molecules due to inclusion complex, resulting in improved drug loading and delayed drug release. On the other side, disulfide bond endows gel backbone with redox sensitivity that can accelerate drug release after the initial rapid drug release by opening the disulfide bond using glutathione solution and avoid incomplete drug release. Two potential ophthalmic drugs, puerarin and curcumin, were used as model drugs to evaluate the drug loading, release properties and redox sensibility of the cyclodextrin-grafted redox-responsive hydrogel mediated by disulfide bond.

## 2. Materials and methods

### 2.1. Materials

Acetic anhydride ( $\text{AC}_2\text{O}$ , 99%), 2,2'-disulfanediyldiacetic acid (96%), 4-dimethylaminopyridine (DMAP), 2-hydroxyethyl methacrylate (HEMA), reduced glutathione (GSH) and 1-(3-dimethylaminopropyl)-3-ethylcarbodiimide hydrochloride (EDC, 99%) were purchased from Sinopharm Chemical Reagent Co. N-Hydroxysulfosuccinimide sodium salt (NHS,99%),  $\beta$ -cyclodextrin ( $\beta$ -CD), 2,2'-azobis (AIBN), Ethylene dimethacrylate (EDGMA), tosyl chloride (p-TsCl) and ethylenediamine (EDA) were purchased from Aladdin

Reagent Co. Puerarin (PUE) was provided by Jiangsu Tiansheng Pharmaceutical Co., Curcumin(CUR) was purchased from Hubei Changao Pharmaceutical Co. Tween 80 (99%) and Cell Counting Kit-8 (CCK-8) were purchased from Shanghai Dibai Biotechnology Co. All other reagents were analytic grade and used as received without further purification.

### 2.2. Synthesis of mono-methacrylated $\beta$ -cyclodextrin monomer mediated by disulfide bond

First, Mono-EDA- $\beta$ -CD was synthesized by a two-step reaction according to previously published articles [32]. Then, NHS ester functional monomer was synthesized according to previous report [33]. Finally, NHS ester functional monomer (3.93 g, 10 mmol) and mono-EDA- $\beta$ -CD (2.9 g, 2 mmol) were dissolved in 20 mL DMSO and stirred at 25°C for 3 days. A yellow precipitate is obtained by adding 500 mL acetone to the solution at the end of the reaction. And then, the precipitate was repeatedly dissolved in the water-methanol mixture, and were precipitated in acetone several times for removal of unreacted components. The precipitate was dried under vacuum at 30°C overnight to obtain mono-methacrylated  $\beta$ -cyclodextrin monomer mediated by disulfide bond (MA-SS- $\beta$ -CD, 2.5 g).

### 2.3. Preparation of redox-responsive hydrogel film

Monomer of MA-SS- $\beta$ -CD, cross-linker of EDGMA (0.2 wt % of total monomers) and initiator of AIBN (0.2 wt% of total monomers) were dissolved in 50 mg solvent of DMSO, in which monomer of HEMA were added followed by sonicating for 1 min to obtain transparent polymerization solution. Then, the polymerization solution was injected into the cavity of a polypropylene plate mold separated by a polypropylene frame with a thickness of 200  $\mu\text{m}$  and then cured at 80°C for 12 h. Finally, transparent redox-responsive hydrogel films were immersed in ultra-pure water at 25°C for 48 h to remove solvent of DMSO. Subsequently, all hydrogel films were freeze-dried for 48 h to ensure the complete removal of DMSO.

### 2.4. Characterization

#### 2.4.1. $^1\text{H}$ NMR and $^{13}\text{C}$ NMR spectroscopy

The  $^1\text{H}$  NMR and  $^{13}\text{C}$  NMR analyses of mono-EDA- $\beta$ -CD, NHS ester functional monomer, and mono-methacrylated  $\beta$ -cyclodextrin monomer mediated by disulfide bond

(MA-SS- $\beta$ -CD) were carried out on a Bruker AC (400 MHz) spectrometer using DMSO- $d_6$  as solvent.

#### 2.4.2. Fourier transform infrared spectroscopy (FTIR)

The FTIR spectra of mono-EDA- $\beta$ -CD, NHS ester functional monomer, and MA-SS- $\beta$ -CD monomer were recorded on an IR Prestige-21 over the range 400–4000  $\text{cm}^{-1}$  using the potassium bromide pellet technique.

#### 2.4.3. Element analysis

All samples had been subjected to the soxhlet extraction treatment using 80 mL of ethanol as the extractant for 12 h before testing, and then all samples were dried at 105°C for 12 h. The content of C, N, H, S in mono-methacrylated  $\beta$ -cyclodextrin monomer and the redox-responsive hydrogel were directly determined on a Vario EL III instrument. The content of  $\beta$ -CD in the hydrogels was calculated according to the content of S element.

#### 2.4.4. Gel fraction

Polymerizable solution (monomers of HEMA and MA-SS- $\beta$ -CD, crosslinker of EGDMA) with a total weight of  $W_0$  and initiator of AIBN, solvent of DMSO were mixed and injected into molds. After 12 h curing at 80°C, the molds were opened and curing hydrogel films were taken out and wrapped in a filter paper, and then Soxhlet extraction was carried out with 80 mL anhydrous ethanol as the extraction solution for 12 h. The gel film by Soxhlet extraction were dried at 105°C for 12 h, and then weight ( $W_1$ ). The gel fraction (%) was calculated according to Equation (1).

$$\text{Gel fraction}(\%) = \frac{W_1}{W_0} \times 100\% \quad (1)$$

#### 2.4.5. UV-Visible absorption/transmittance spectra

The hydrated redox-responsive hydrogel films with different content of MA-SS- $\beta$ -CD were cut into  $10 \times 30 \text{ mm}^2$  strips and attached to the inner wall of quartz cuvettes filling with ultra-pure water, and its absorbance/transmittance spectra were measured by Agilent Cary 60 Spectrophotometer over the range of 200–800 nm using ultra-pure water as a reference.

#### 2.4.6. Equilibrium swelling degree (ESD)

The hydrated hydrogel films with different MA-SS- $\beta$ -CD contents were cut into  $10 \times 30 \text{ mm}^2$  and wiped with filter paper to remove its surface water. The hydrated hydrogel strips ( $W_{t0}$ ) were placed in an oven at 37°C, and their weights ( $W_t$ ) were measured at different dehydration times within 2 h. Finally, the temperature of the oven was raised to 105°C for 2 h to obtain dried hydrogel

( $W_d$ ), and the equilibrium swelling degree (ESD) of the hydrogel was calculated according to Equation (2):

$$\text{ESD}(\%) = \frac{W_{t0} - W_d}{W_{t0}} \times 100\% \quad (2)$$

where  $W_{t0}$  and  $W_d$  represent the weight of hydrogel in swelling state and dry state, respectively.

#### 2.4.7. Differential scanning calorimetry (DSC)

Differential scanning calorimetry (DSC) analyses were carried out on a DSC-25 Waters TA Instruments calorimeter with a TA Universal Analysis 2000 software. All operations were carried out in a nitrogen atmosphere. The hydrated hydrogel films about 8 mg were put in aluminum sample pans. The samples were cooled down to  $-40^\circ\text{C}$  and heated up to  $40^\circ\text{C}$  at a rate of  $5^\circ\text{C}/\text{min}$ . Both quantitative and qualitative data on endothermic processes were obtained from the thermograms. Measure three times in parallel, and then the free ( $X_{\text{free}}$ ) and bound water ( $X_{\text{bound}}$ ) content in the hydrogels were calculated using the following formula [34,35].

$$X_{\text{free}} = \frac{H_m}{H_f} \times 100\% \quad (3)$$

$$X_{\text{bound}} = X_{\text{total}} - X_{\text{free}} \quad (4)$$

where  $H_m$  is the melting enthalpy of tested lenses and  $H_f$  is the heat of fusion of pure water (340.6 J/g).

#### 2.4.8. Mechanical properties

The WDN-05J universal testing machine was used to test the mechanical properties of different hydrated hydrogels at room temperature and a relative humidity of 60%. The hydrated hydrogel films with a thickness of 200  $\mu\text{m}$  were cut into  $10 \times 30 \text{ mm}^2$  strips and tested in triplicate with a crosshead speed of 20  $\text{mm}\cdot\text{min}^{-1}$ .

#### 2.4.9. Cytocompatibility

The UV-sterilised hydrogel film ( $10 \times 10 \text{ mm}^2$ ) was immersed in 500  $\mu\text{L}$  of DMEM high glucose medium with 10 vol% FBS for 24 h to obtain the extraction medium. L929 cells were inoculated into 96-well plates ( $5 \times 10^4$  cells/well, 500  $\mu\text{L}$ ) and incubated at 37°C for 24 h. The culture medium was replaced with 100  $\mu\text{L}$  of extraction medium and incubated at 5%  $\text{CO}_2$  for 24 h at 37°C. To investigate the cellular activity using the CCK-8 assay, the CCK-8 stock solution was added into the PBS solution to obtain the final CCK-8 assay (5 mg/mL in PBS), and the culture medium was removed from the culture medium and gently rinsed with PBS for two times. Then, 10  $\mu\text{L}$  of

CCK-8 assay solution was added to the the cell-seeded samples and incubate further for 4 h, and then 100  $\mu$ L DMSO was added. Optical density (OD) was measured using a spectrophotometric plate reader (Spectra Max M5) at a wavelength of 450 nm. Cell viability (%) of the samples was calculated using Equation (5):

$$\text{Cellviability}(\%) = \frac{OD_{\text{sample}}}{OD_{\text{control}}} \times 100\% \quad (5)$$

#### 2.4.10. Drug loading

Hydrated hydrogel films ( $10 \times 30 \text{ mm}^2$ ) were dried at  $105^\circ\text{C}$  for 12 h, and then immersed in 10 ml aqueous soaking solutions with puerarin (PUE) concentrations of  $0.8 \text{ mg}\cdot\text{ml}^{-1}$  or ethanol soaking solutions with curcumin (CUR) concentrations of  $1.0 \text{ mg}\cdot\text{ml}^{-1}$  to load drug for 48 h. The concentration of soaking solutions after drug loading was determined at the maximum absorption wavelength of 250 nm (PUE) and 425 nm (CUR) using an Alpha-1502 spectrophotometer. The amount of loaded drug on the hydrogel was calculated as the difference of drug mass in soaking solution.

#### 2.4.11. In vitro drug release

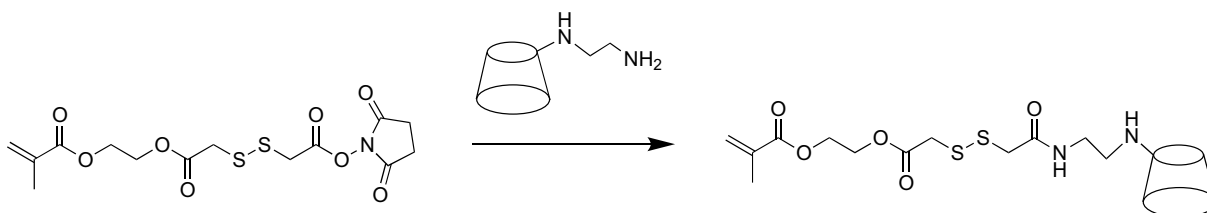
The hydrogel films loaded with PUE or CUR were immersed in 100 ml release medium of 0.01 M PBS-T buffer solution ( $\text{pH}=7.4$ ) or PBS solution ( $\text{pH}=7.4$ , 0.01 M) containing 1.5 wt.% Tween 80, respectively, and then shaken at 120 rpm at  $37^\circ\text{C}$ . A sample of 5 ml of release medium was taken out and replaced with the same volume of fresh release medium at regular time intervals in order to mimic perfect sink conditions for release evaluation. The concentration of PUE or CUR in the release medium was determined using an UV-vis spectrophotometer. To evaluate the redox responsive of the hydrogels, different concentration of GSH was added to release medium. In addition, we have conducted drug release studies on the films at different pH conditions, and the release behavior of drug loaded hydrogel was determined as above.

### 3. Results and discussion

#### 3.1. Synthesis of mono-methacrylated $\beta$ -cyclodextrin monomer mediated by disulfide bond (MA-SS- $\beta$ -CD)

Mono-EDA- $\beta$ -CD and NHS ester functional monomer with chemical structure shown in Scheme 1 were firstly synthesized, and then dissolved all in DMSO to react as the route shown in Scheme 1 to synthesize mono-methacrylated  $\beta$ -cyclodextrin monomer mediated by disulfide bond.  $^1\text{H}$  NMR spectra of the raw materials and the product are shown in Figure 1. The peaks at 2.70 ppm in Figure 1b are attributed to  $-\text{CH}_2$  adjacent to primary and secondary amines. The characteristic peaks of  $\beta$ -CD were observed at 3.68–3.83 ppm, 3.25–3.51 ppm, 4.85 ppm, and 5.75 ppm corresponding to the protons in sugar units of  $\beta$ -CD. The peak of  $-\text{CH}_2$  adjacent to the disulfide bond in the functional monomers of NHS ester (Figure 1a) appeared at 3.62 and 3.78 ppm, which overlapped with the  $\beta$ -CD characteristic peaks, making it difficult to determine whether the disulfide bond was grafted onto  $\beta$ -CD or not. However, the characteristic peak of the  $\text{CH}_2=\text{CH}_2$  appears at 5.53 ppm and 6.05 ppm and is not interfered by other peaks. In the spectrum of SS- $\beta$ -CD (Figure 1c), the signal peaks of the proton of  $=\text{CH}_2$  at 6.05 ppm and the three major absorption peaks of  $\beta$ -CD at 3.68–3.83 ppm, 3.25–3.51 ppm, 4.85 ppm and 5.75 ppm can be observed simultaneously, so it can be determined that the disulfide bond is successfully grafted to  $\beta$ -CD. Moreover, the peak area ratio between the peak at 6.05 ppm and the peak at 4.85 ppm is 1:7, and the content of S element in the monomer is 4.39% as shown in the element results shown in Table 2. This is in agreement with calculated S content (4.40%) on the basis of molecular formula indicating that only one polymerizable carbon-carbon double bond was grafted onto  $\beta$ -CD and mono-methacrylated  $\beta$ -cyclodextrin monomer was successfully synthesized.

$^{13}\text{C}$  NMR spectra of the intermediates and MA-SS- $\beta$ -CD are shown in Figure 2. Absorption peaks located at 102.7, 82.04, 72.5–73.8, 60.5, and 31.2 ppm which are attributable to  $\beta$ -CD can be observed in Figure 2b, and



**Scheme 1.** The synthesis route of mono-methacrylated  $\beta$ -cyclodextrin monomer mediated by disulfide bond.



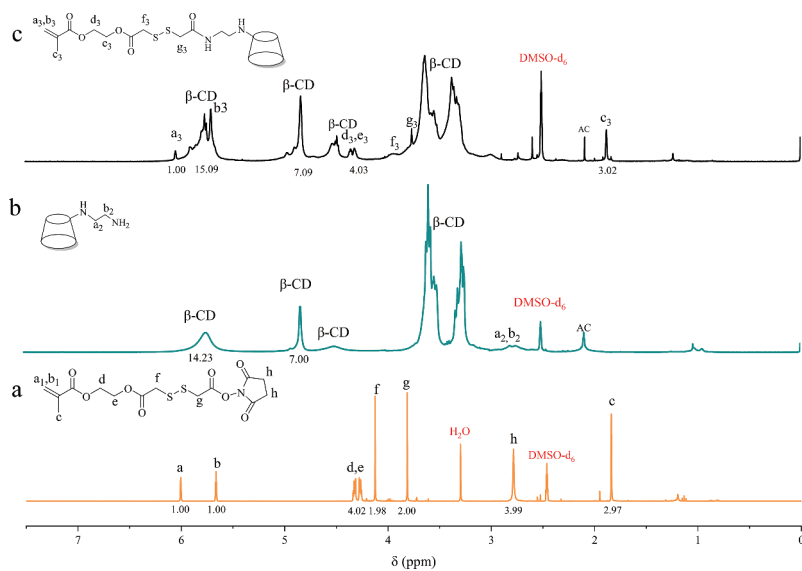


Figure 1. The  $^1\text{H}$  NMR spectra of intermediates and MA-SS- $\beta$ -CD.

Table 2. Gel fraction and element content of the MA-SS- $\beta$ -CD monomer and dried hydrogels.

Samples	Gel fraction (wt%)	Element content (wt.%)				$\beta$ -CD content (wt.%)
		N	C	H	S	
Monomer		2.05	41.71	6.03	4.39	77.85
2	92.7	0.07	53.74	6.8	0.15	2.66
3	89.0	0.22	53.38	6.89	0.31	5.68
4	85.2	0.3	52.89	6.75	0.5	8.87
5	83.5	0.42	52.98	6.82	0.78	13.83

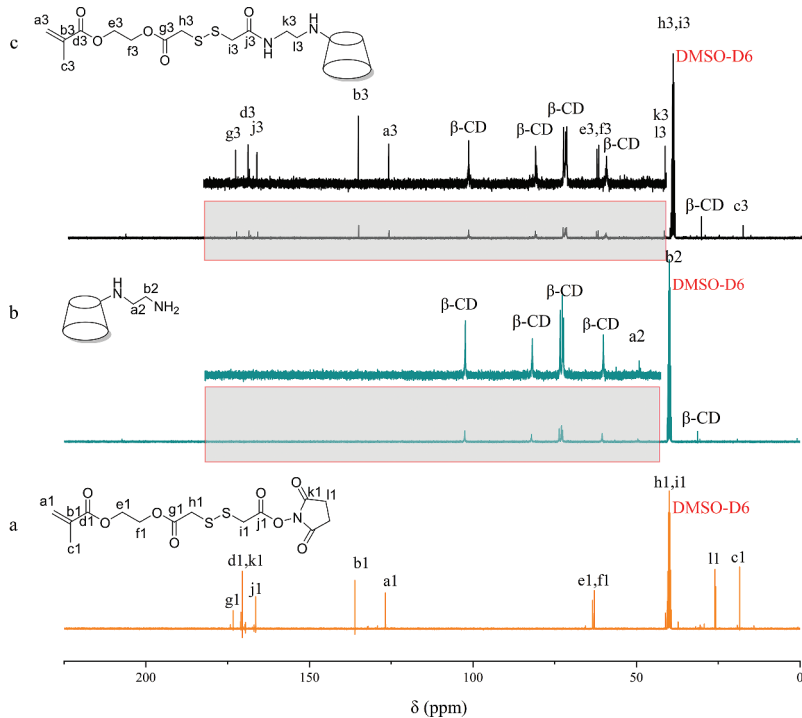
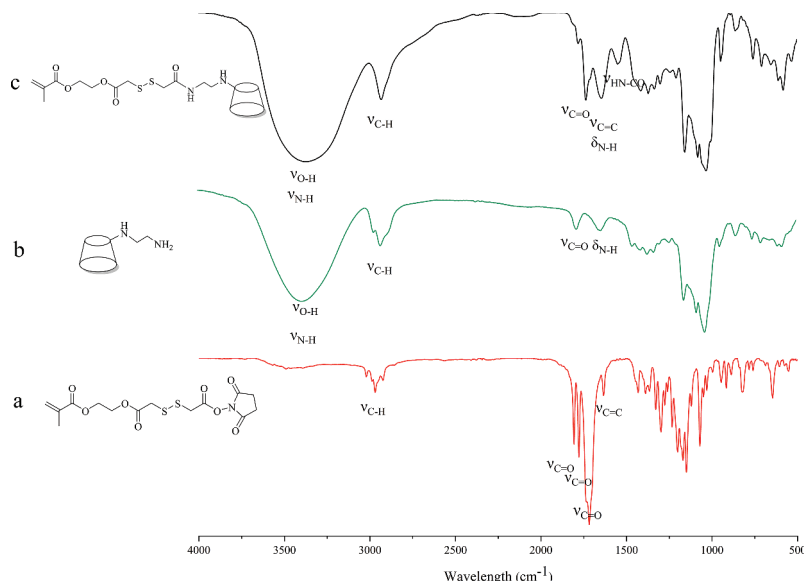


Figure 2. The  $^{13}\text{C}$  NMR spectra of intermediates and MA-SS- $\beta$ -CD.



**Figure 3.** The FTIR spectra of intermediates and MA-SS- $\beta$ -CD.

a signal peak for the carbon atom in  $-\text{CH}_2$  of the EDA is also present at 49.5 ppm. In **Figure 2a**, signal peaks at 173.2, 170.1, and 166.4 ppm caused by four different C=O can be observed. The absorption peaks due to the  $\text{CH}_2=\text{CR}_1\text{R}_2$  in the HEMA fragment and the  $-\text{CH}_2$  in the NHS fragment can be seen at 126.7 and 26 ppm. In the spectrum of the final product, characteristic peaks induced by C=O as well as  $\text{CH}_2=\text{CR}_1\text{R}_2$  can be seen, and the disappearance of the absorption peak located at 26 ppm is due to the cleavage of the NHS fragment. Moreover, the  $-\text{CH}_2$  absorption peak of EDA, which was originally located at 59.5 ppm, was shifted due to the

formation of amide bonds. It can be concluded that we have successfully synthesized the MA-SS- $\beta$ -CD.

**Figure 3** shows FTIR spectra of intermediates and the final product of MA-SS- $\beta$ -CD. The absorption peak centered at  $1650\text{ cm}^{-1}$  is related to the C=C and N-H stretching vibration. The absorption peak centered at  $1780\text{ cm}^{-1}$  is attributed to the C=O stretching vibration, and the absorption band around  $2920\text{--}3010\text{ cm}^{-1}$  can be ascribed to C-H stretching vibration affected by the adjacent groups. The spectrum of the final product (**Figure 3c**) was similar to that of EDA- $\beta$ -CD, but there was an absorption peak at  $1550\text{ cm}^{-1}$  due to stretching

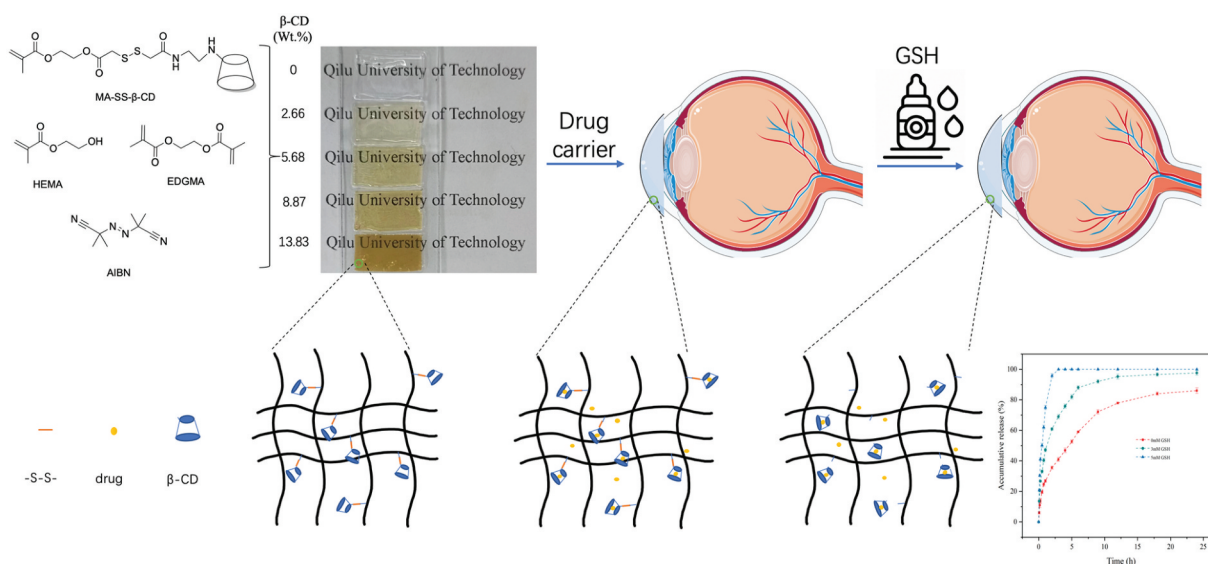


**Figure 4.** Schematic diagram of redox-responsive hydrogel backbone and regulated drug release by GSH drops.

vibrations of HN-CO in the amide II band, which concluded that the disulfide bond was successfully grafted on  $\beta$ -CD.

### 3.2. Preparation and characterization of redox-responsive hydrogel films

As the schematic diagram shown in Figure 4, a redox hydrogel was designed to expect for ocular drug delivery with stable drug release by drop GSH eye drop after initial burst release. Mono-methacrylated  $\beta$ -CD monomer (MA-SS- $\beta$ -CD) is insoluble in 2-hydroxyethyl methacrylate (HEMA), and therefore DMSO was used as solvent. Transparent hydrogels were prepared by

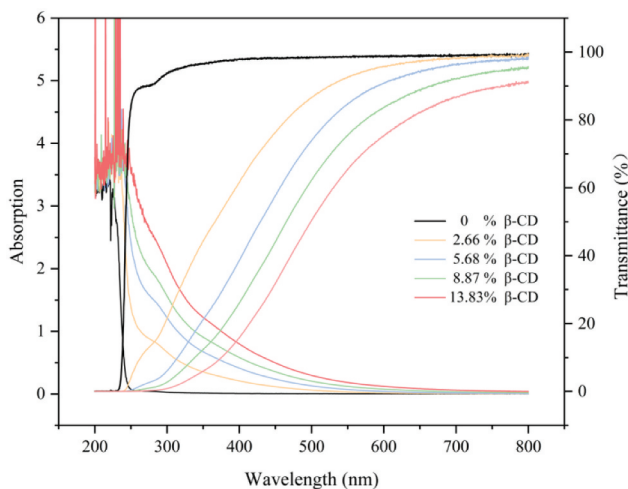


**Figure 5.** The absorbance and transmittance of hydrogel films with different  $\beta$ -CD content.

thermal curing. The MA-SS- $\beta$ -CD monomer can well copolymerize with HEMA monomer with gel fraction over 80% as listed in Table 2. The element content of the hydrogels was determined by element analysis, and  $\beta$ -CD content of the hydrogels was calculated according to its S content (Table 2).

HEMA-based hydrogel film has high visible light transmittance and has been used as contact lens for ophthalmic drug delivery vehicle [36,37]. Figure 5 shows that the transmittance of the hydrogel decreases as the content of MA-SS- $\beta$ -CD component increases. This may be ascribed to the polarity difference between MA-SS- $\beta$ -CD and HEMA, resulting in slightly microphase separation in the hydrogels. The transmittance of the gel film with 13.83%  $\beta$ -CD content remains about 80% at the most sensitive wavelength of the human eye is 600 nm [38], meeting the requirements of light transmission as a therapeutic contact lens material for ophthalmic drug delivery carriers.

Water in hydrogel can be classified by free water and bound water content. The former plays an important role in material transfer such as oxygen and drug transfer between the hydrogel and the external environment, and the latter affects the moisturizing properties of the hydrogels [34,39]. Figure 6a shows water loss curve of hydrated hydrogels at 37°C temperature. All hydrogels undergo a rapid dehydration in the first hour, indicating the presence of a large amount of free water in the hydrogel. Figure 6b shows the equilibrium swelling degree (ESD) of the hydrogel films that positively correlated with the content of  $\beta$ -CD, e.g., the ESD increased from 36.2% to 54.4% as the content of  $\beta$ -CD was

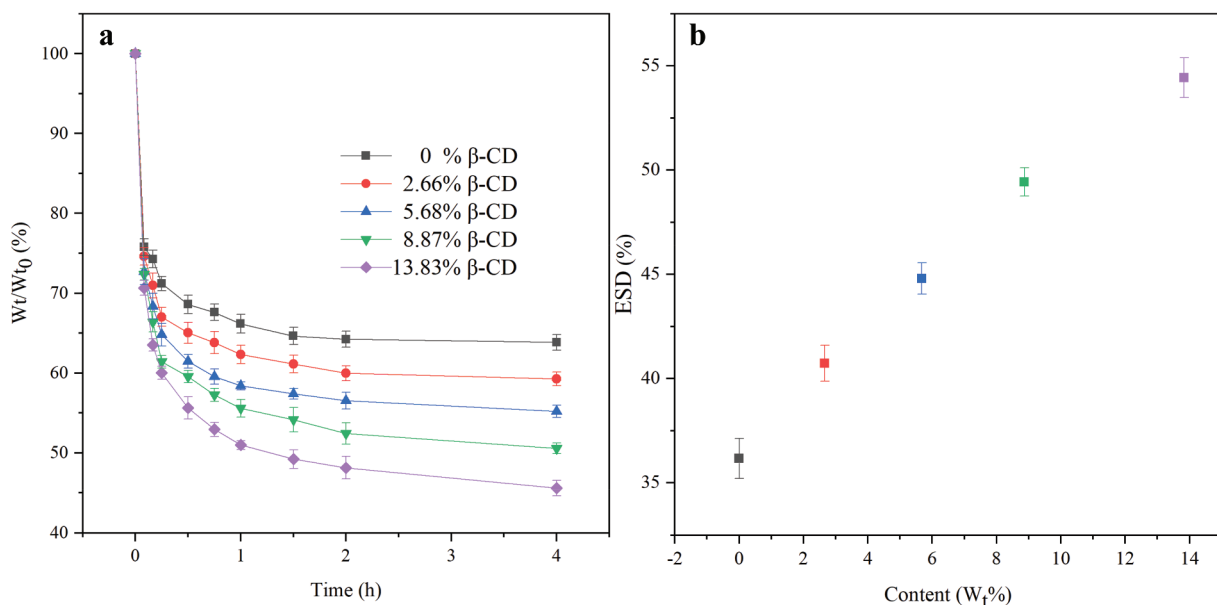


**Figure 6.** The weight loss curves (a) and ESD (b) of hydrogel films with different  $\beta$ -CD content.



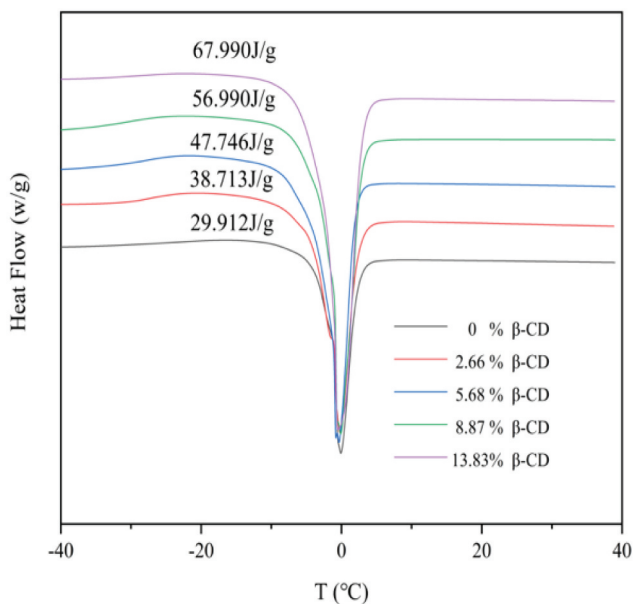


**Figure 7.** The DSC thermograms of hydrogel films with different  $\beta$ -CD contents.

increased from 0% to 13.83%, which can be explained by the multiple hydroxyl groups on  $\beta$ -CD forming hydrogen bonds with water molecules. The existence form of water in the hydrogels was studied by DSC analysis, and the results are shown in Figure 7 and Table 3. All hydrogels show a narrow heat absorption peak at 0°C corresponding to the heat absorption and melting of the frozen free water in the hydrogels. Heat flow gradually increases as the increment of  $\beta$ -CD component in the hydrogels. The proportion of free and bound water in hydrated hydrogel was calculated according to the heat flow and the results are listed in Table 3. It can be seen that the contents of free and bound water were all positively correlated with the contents of CD in the gel. This might be related to the molecular structure of  $\beta$ -CD. One side,  $\beta$ -CD molecules have strong rigidity, and the space between two  $\beta$ -CD molecules can accommodate more water molecules, which leads to an increase in the free water content. On the other side, the multiple hydroxyl groups on  $\beta$ -CD can form non-covalent hydrogen bond forces, resulting in an increment in the bound water content.

**Table 3.** The melting enthalpy and total water content of the hydrogels with different  $\beta$ -CD content and calculated free/bound water.

Samples ( $\beta$ -CD content, wt%)	The melting enthalpy $H_m$ (J/g)	Total water content (wt.%)	Free water content (wt.%)	Bound water content (wt.%)
1 (0)	29.912	36.2	8.78	27.42
2 (2.66)	38.713	40.7	11.37	29.33
3 (5.68)	47.746	44.8	14.02	30.78
4 (8.87)	56.790	49.44	16.67	32.77
5 (13.83)	67.990	54.4	19.96	34.44

Figure 8 shows the stress-strain curves of the hydrogel films with different  $\beta$ -CD content. It is evident that the mechanical properties including in Young's modulus, tensile strength, and elongation at break show an overall increased tendency with the increment of  $\beta$ -CD content. For example, the tensile strength and elonga-

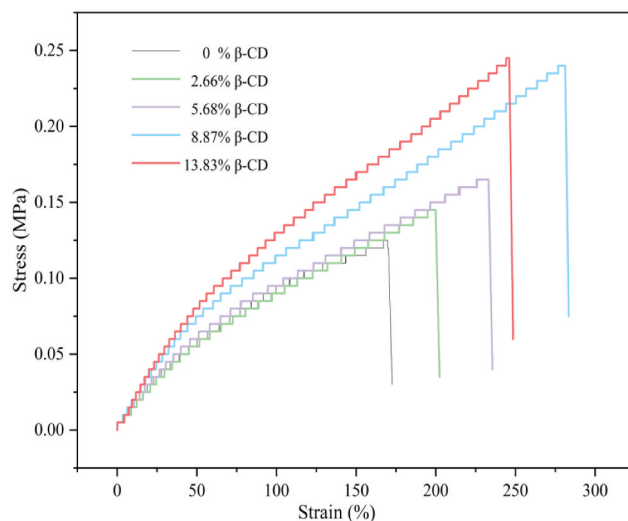


**Figure 8.** Tensile stress-strain curves of wetted hydrogel films with different  $\beta$ -CD content.

tion at break increased from the original 0.125 MPa and 169.9% to 0.239 MPa and 281.2% with the increase of  $\beta$ -CD content from 0 to 8.87%. This may be ascribed to rigid  $\beta$ -CD molecule with abundant hydroxyl forming more intermolecular hydrogen bonds [40,41] or the subject-guest interactions between  $\beta$ -CD and some smaller polymer fragments interspersed in the cavities of  $\beta$ -CD [42,43]. These results show that the hydrogel films containing  $\beta$ -CD both exhibit better tensile properties than the pure HEMA hydrogel films, indicating that the hydrogel film with  $\beta$ -CD has better flexibility. pHEMA hydrogel has been widely used as contact lens, and incorporation of  $\beta$ -CD in the hydrogels may improve its movement during blinking because of higher Young's modulus [44].

To verify the biocompatibility of hydrogels with different percentages of  $\beta$ -CD, cytotoxicity test was carried out using L929 cells (Figure 9). The results show that the

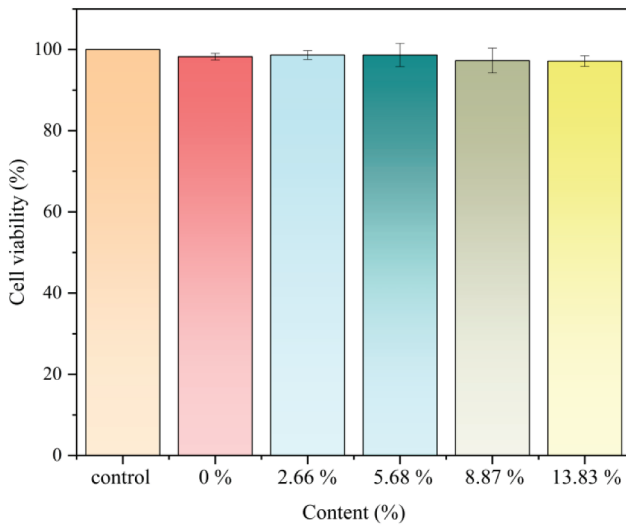


**Figure 9.** Cytotoxicity assay of hydrogel films with different  $\beta$ -CD content.

cell viability after treatment with hydrogels containing 0%, 2.66%, 5.68%, 8.87%, and 13.83% of  $\beta$ -CD was 98.24%, 98.65%, 98.65%, 97.29%, and 97.15%. This indicates that the redox-responsive hydrogels have low cytotoxicity, and it can be used as a medical biomaterial.

### 3.3. Drug loading and in vitro release

Two drugs, PUE and CUR, are used as model drugs for drug loading tests, and the results are shown in Figure 10a,b. It can be observed that the drug-loading capacity of the hydrogel is directly proportional to content of  $\beta$ -CD, indicating that two drugs can all form

inclusion complexes with the hydrophobic  $\beta$ -CD cavity. The hydrogel films containing  $\beta$ -CD show a large difference in loading capacity for PUE and CUR, and the average increased loaded amount of CUR is about 3.85 mg/g dried hydrogels, significantly greater than increased PUE loaded amount (1.15 mg/g dried hydrogels) as every 10% increment of added free MA-SS- $\beta$ -CD content.  $\beta$ -CD forming complexes with PUE and CUR accounted for 10.78 wt% and 35.01 wt%, respectively, calculated according to Equation (6) [45]. This indicates that the loading amount can be further improved. The drugs forming inclusion complexes with  $\beta$ -cyclodextrin accounted for 49.72% and 89.36%, respectively, of total loaded PUE and CUR calculated by Equation (7) [44], indicating that  $\beta$ -CD component in the hydrogel significantly improved the drug-loading capacity.

$$X_{inclusion} = \frac{[m_{pHEMA/\beta-CD} - m_{pHEMA}(1 - C_{\beta-CD})] \times M_{\beta-CD}}{1000 \times C_{\beta-CD} \times M_{drug}} \quad (6)$$

$$X_{free} = \frac{m_{pHEMA} \times (1 - C_{\beta-CD})}{m_{pHEMA/\beta-CD}} \times 100\% \quad (7)$$

where  $m_{pHEMA}$  and  $m_{pHEMA/\beta-CD}$  are the amounts of loaded drug (mg) in 1 g dried pHEMA and pHEMA/ $\beta$ -CD hydrogel, respectively,  $M_{\beta-CD}$  and  $M_{drug}$  are the molecular weight of  $\beta$ -CD (1135 Da) and the drug (PUE, 416 Da; CUR, 368 Da), respectively, and  $C_{\beta-CD}$  is the actual content of  $\beta$ -CD (about 13.83 wt.%) in the hydrogel film.

The drug release rate is governed by diffusion of free drug in aqueous phase of the hydrogel, dissociation of  $\beta$ -CD/drug molecule inclusion complexes, and absorbed drug by pHEMA backbone. All hydrogels show burst release of drug at initial release time as

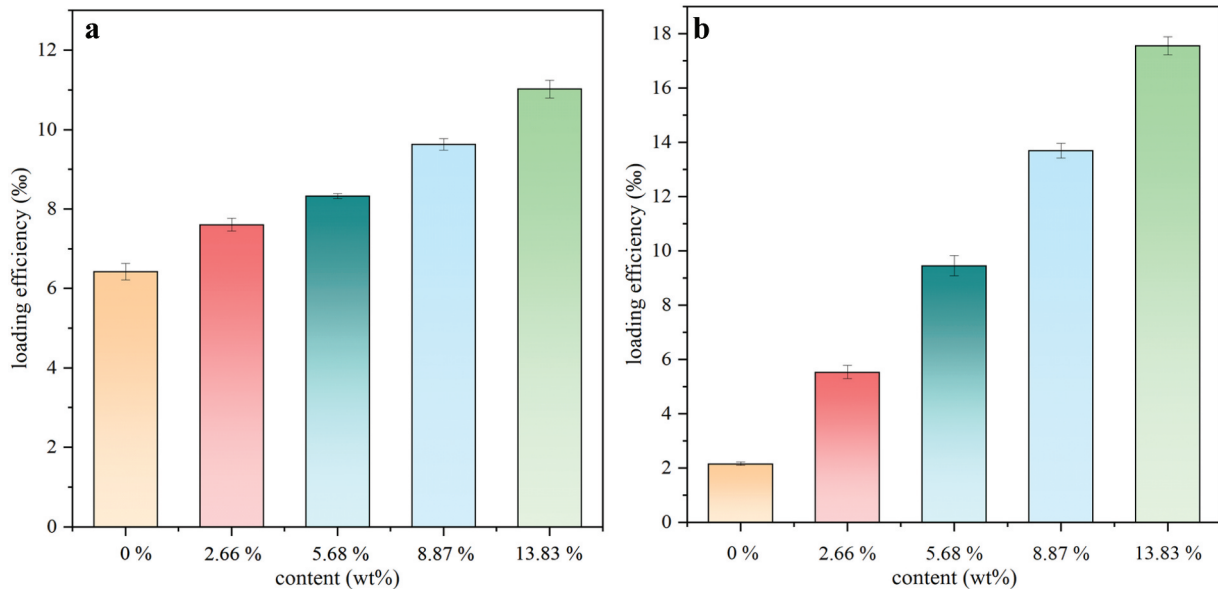


**Figure 10.** Loading capacity of gel films with different ratios for (a) PUE and (b) CUR.

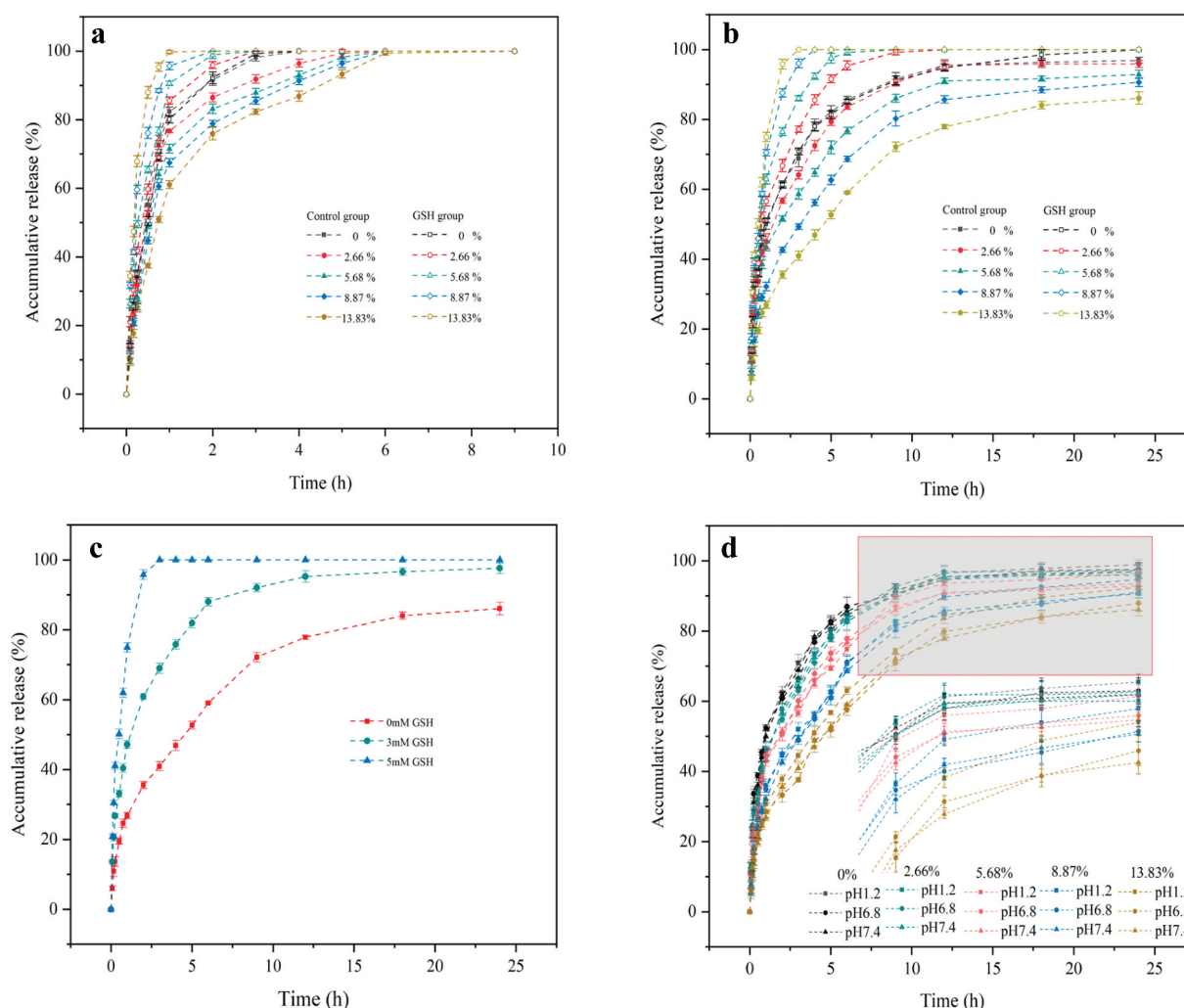


**Figure 11.** Drug release profiles of hydrogel films with different ratios of MA-SS-β-CD loaded with (a) PUE and (b) CUR under non-redox and redox conditions. (c) Drug release profiles of CUR-loaded hydrogel films under different redox conditions. (d) Drug release profiles of CUR-loaded hydrogel films under different pH conditions.

shown in Figure 11a and 11b, and more than 60% PUE (Figure 11a) and 25% CUR (Figure 11b) are released from the hydrogels in 1 h. Moreover, the incorporation of β-CD in the hydrogel decreases its burst release effect. This indicates that free drugs in aqueous phase and absorbed drug by HEMA backbone can be rapidly release from the hydrogels, resulting in burst release, and the following sustain release is mainly ascribed to higher affinity from inclusion complex between drug and β-CD. Figure 11 shows that PUE can be completely released into release medium in 6 h, while about 20% loaded CUR was still not released within 24 h, especially the hydrogel with high β-CD content. Burst release is a main problem for hydrogel drug delivery. This can be overcome by improved affinity between drug and the polymer backbone in the hydrogel. However, high affinity often leads to Incomplete drug release, resulting in drug loss and

difficulty in achieving long-term therapeutic effects as shown in the hydrogel incorporating β-CD for CUR delivery. It is obviously important to improve the release rate of high affinity drug in its release later stage from hydrogel. Based on this, we designed the hydrogel backbone: linking β-CD molecule onto polymer backbone by disulfide bonds that can be broken in a reducing environment, so as to rapid release of the drug as inclusion state by added GSH. To confirm this, blank hydrogel film was immersed in 3 mM GSH solution for 2 h, and then the sulfur content in the hydrogel was determined. The results showed that the sulfur content decreased from initial 0.78 wt% to 0.43 wt%, indicating that nearly 90% of the disulfide bonds were broken, and the hydrogel shows high redox sensitivity to GSH.

The effect of GSH on drug release was studied and the results are shown as GSH group in Figure 11a,b.

GSH improves strongly drug release rate from  $\beta$ -CD-containing hydrogels. The higher the content of  $\beta$ -CD in the hydrogel, the faster the drug release rate, resulting in both PUE and CUR can be completely release in 5 h under redox conditions provided by GSH. This was mainly ascribed to rapidly diffuses of GSH into the gel matrix, and then reducing disulfide bonds into sulfhydryl groups, and  $\beta$ -CD and included drug were dissociated from the hydrogel backbone, and then release into release medium. Figure 11c shows the drug release curves of the hydrogels under different different redox conditions provided by different GSH concentration in release medium. It can be seen that more than 80% of loaded drug was released in 5 h at low GSH concentration of 3 mM, indicating that the hydrogel system was highly sensitive to GSH and only a small amount of GSH was required to significantly accelerate the drug release. This suggests that the hydrogel may be suitable as a drug loading contact lens for ocular drug delivery. After the drug release, GSH eye drops are dosed to accelerate the release of residual curcumin, so as to maintain a longer and smoother drug concentration in tears. In addition, released  $\beta$ -CD possess a thiol group from broken disulfide bonds, which can bind with the amino acid residues of eye proteins, resulting in a perhaps increased residence times of the drug in the eyes [46].

The drug release profiles of pure pHEMA gel film and gel films with different  $\beta$ -CD content at pH 1.2, 6.8, and 7.4 are shown in Figure 11d. It can be seen that the release profiles of the pHEMA film and the gel films with different  $\beta$ -CD content at pH 7.4 and 6.8 remain basically unchanged, which demonstrates that the gels are more stable in neutral and weak acidic environments. The 24-h cumulative release of the pHEMA film at pH 1.2 was only about 1.7% higher than at pH 7.4, which was not a significant improvement. Whereas, the 24-h cumulative release of the gel film with 13.83%  $\beta$ -CD content increased by about 6.4% at pH 1.2. The reason for this phenomenon is that the ester bond in the gel network is hydrolyzed under strongly acidic conditions. This occurs as a minor disruption for the pHEMA gel network, whereas for gel films containing MA-SS- $\beta$ -CD (containing ester bond), ester bond breakage results in the release of the inclusion complexes. Figure 11d shows that the more apparent hydrolysis of the ester bond occurs after about 9 h, whereas in Figure 11c, a large number of disulfide bond breaks in gel film with 13.83%  $\beta$ -CD content can be observed within 9 h under 3 mM GSH conditions. This indicates that the gel film is stable to acid and the gel is more sensitive to GSH compared to acid.

To predict and clarify the drug release *in vitro*, the results should be fitted with a suitable mathematical model. We used four mathematical models, including the Zero-order (8), First-order (9), Higuchi (10), and Korsmeyer-Peppas (11) models, to clarify the mechanism of drug release from the hydrogel film. We found that the first-order and Korsmeyer-Peppas models fitted better, and their  $R^2$  was above 0.91 (Supporting information). The diffusion exponent ( $n$ ) in the Korsmeyer-Peppas fitted model was below 0.45, which indicated that all the drug release mechanisms were fick diffusion. Interestingly, the diffusion exponent ( $n$ ) of curcumin was higher in the 5 mM GSH condition than in the non-GSH condition, demonstrating that the drug release is inclined to be the combination of diffusion and erosion. The reasons for this are the high affinity of  $\beta$ -CD for curcumin and the high sensitivity of the disulfide bond to GSH.

$$\frac{M_t}{M_\infty} = K_z t \quad (8)$$

$$\frac{M_t}{M_\infty} = a(1 - e^{-K_f t}) \quad (9)$$

$$\frac{M_t}{M_\infty} = -K_h t^{\frac{1}{2}} \quad (10)$$

$$\frac{M_t}{M_\infty} = K_p t^n \quad (11)$$

## Conclusions

Mono-methacrylated  $\beta$ -cyclodextrin ( $\beta$ -CD) monomer mediated by disulfide bond was synthesized, and redox-responsive hydrogel incorporating  $\beta$ -CD were successfully prepared. The hydrogels have good biocompatibility, high light transmittance, and excellent mechanical properties. Incorporation of  $\beta$ -CD in the hydrogel increases loading amount of puerarin and curcumin by 1.8 and 8.5 folds because of inclusion complexes between drug molecules and  $\beta$ -CD cavity, resulting in slower release rate of two drugs from the hydrogel as shown in the control group in Figure 11a and Figure 11b under non-reducing conditions, especially curcumin release was prolonged more than 24 h from 5 h of pure pHEMA hydrogel (80% release). The disulfide bridge bond between  $\beta$ -CD and main chain of the hydrogel backbone is highly sensitive to reduced glutathione (GSH), and low GSH concentration of 3 mM can break the disulfide bond, resulting in rapid release of  $\beta$ -CD/drug complexes. The redox-responsive hydrogel has potential application as contact lenses loaded drugs with high affinity to cyclodextrin for ocular drug delivery.

## Disclosure statement

No potential conflict of interest was reported by the author(s).

## Funding

This work was supported by the National Natural Science Foundation of China [Nos. 22178184], the Shandong Provincial Natural Science Foundation, China [Nos. ZR2021MB007], by Science, Education and Industry Integration Innovation Pilot Project from Qilu University of Technology (Shandong Academy of Sciences) [2022JBZ02-04], and Program for Scientific Research Innovation Team in Colleges and Universities of Shandong Province.

## Data availability statement

The authors confirm that the data supporting the findings of this study are available within the article.

## References

- [1] Zhong D, Tu Z, Zhang X, et al. Bioreducible peptide-dendrimeric nanogels with abundant expanded voids for efficient drug entrapment and delivery. *Biomacromolecules*. 2017;18(11):3498–3505. doi: [10.1021/acs.biomac.7b00649](https://doi.org/10.1021/acs.biomac.7b00649)
- [2] Zhang R, Li X, He K, et al. Preparation and properties of redox responsive modified hyaluronic acid hydrogels for drug release. *Polym Adv Technol*. 2017;28(12):1759–1763. doi: [10.1002/pat.4059](https://doi.org/10.1002/pat.4059)
- [3] Feng N, Yang M, Feng X, et al. Reduction-responsive polypeptide nanogel for intracellular drug delivery in relieving collagen-induced arthritis. *ACS Biomater Sci Eng*. 2018;4(12):4154–4162. doi: [10.1021/acsbiomaterials.8b00738](https://doi.org/10.1021/acsbiomaterials.8b00738)
- [4] Zhu B, Zong T, Zheng R, et al. Acid and glutathione dual-responsive, injectable and self-healing hydrogels for controlled drug delivery. *Biomacromolecules*. 2024;25(3):1838–1849. doi: [10.1021/acs.biomac.3c01274](https://doi.org/10.1021/acs.biomac.3c01274)
- [5] Li D, Kordalivand N, Fransen MF, et al. Reduction-sensitive dextran nanogels aimed for intracellular delivery of antigens. *Adv Funct Mater*. 2015;25(20):2993–3003. doi: [10.1002/adfm.201500894](https://doi.org/10.1002/adfm.201500894)
- [6] Cao F, Ma G, Mei L, et al. Development of disulfide bond crosslinked antimicrobial peptide hydrogel. *Colloids Surf A Physicochem Eng Asp*. 2021;626:127026. doi: [10.1016/j.colsurfa.2021.127026](https://doi.org/10.1016/j.colsurfa.2021.127026)
- [7] Yao J, Li T, Shi X, et al. A general prodrug nanohydrogel platform for reduction-triggered drug activation and treatment of taxane-resistant malignancies. *Acta Biomaterialia*. 2021;130:409–422. doi: [10.1016/j.actbio.2021.05.047](https://doi.org/10.1016/j.actbio.2021.05.047)
- [8] Roberts MJ, Bentley MD, Harris JM. Chemistry for peptide and protein PEGylation. *Adv Drug Delivery Rev*. 2012;64:116–127. doi: [10.1016/j.addr.2012.09.025](https://doi.org/10.1016/j.addr.2012.09.025)
- [9] Li D, van Nostrum CF, Mastrobattista E, et al. Nanogels for intracellular delivery of biotherapeutics. *J Control Release*. 2017;259:16–28. doi: [10.1016/j.jconrel.2016.12.020](https://doi.org/10.1016/j.jconrel.2016.12.020)
- [10] Cheng R, Yan Y, Liu H, et al. Mechanically enhanced lipo-hydrogel with controlled release of multi-type drugs for bone regeneration. *Appl Mater Today*. 2018;12:294–308. doi: [10.1016/j.apmt.2018.06.008](https://doi.org/10.1016/j.apmt.2018.06.008)
- [11] Osmani BF, Giuliani LM, Reolon JB, et al. Gellan gum-based hydrogel containing nanocapsules for vaginal indole-3-carbinol delivery in trichomoniasis treatment. *Eur J Pharm Sci*. 2020;151:105379. doi: [10.1016/j.ejps.2020.105379](https://doi.org/10.1016/j.ejps.2020.105379)
- [12] Fahr A, Liu X. Drug delivery strategies for poorly water-soluble drugs. *Expert Opin Drug Deliv*. 2007;4(4):403–416. doi: [10.1517/17425247.4.4.403](https://doi.org/10.1517/17425247.4.4.403)
- [13] Gonzalez-Gaitano G, Isasi JR, Velaz I, et al. Drug carrier systems based on cyclodextrin supramolecular assemblies and polymers: present and perspectives. *Curr Pharm Des*. 2017;23(3):411–432. doi: [10.2174/1381612823666161118145309](https://doi.org/10.2174/1381612823666161118145309)
- [14] Liu DE, Chen Q, Long Y-B, et al. A thermo-responsive polyurethane organogel for norfloxacin delivery. *Polym Chem*. 2018;9(2):228–235. doi: [10.1039/C7PY01803G](https://doi.org/10.1039/C7PY01803G)
- [15] Pinelli F, Ponti M, Delleani S, et al.  $\beta$ -cyclodextrin functionalized agarose-based hydrogels for multiple controlled drug delivery of ibuprofen. *Int J Biol Macromol*. 2023;252:126284. doi: [10.1016/j.ijbiomac.2023.126284](https://doi.org/10.1016/j.ijbiomac.2023.126284)
- [16] Boztas AO, Karakuzu O, Galante G, et al. Synergistic interaction of paclitaxel and curcumin with cyclodextrin polymer complexation in human cancer cells. *Mol Pharm*. 2013;10(7):2676–2683. doi: [10.1021/mp400101k](https://doi.org/10.1021/mp400101k)
- [17] Shoukat H, Pervaiz F, Khan M, et al. Development of  $\beta$ -cyclodextrin/polyvinylpyrrolidone-co-poly (2-acrylamide-2-methylpropane sulphonic acid) hybrid nanogels as nano-drug delivery carriers to enhance the solubility of Rosuvastatin: an in vitro and in vivo evaluation. *PLoS ONE*. 2022;17(1):0263026. doi: [10.1371/journal.pone.0263026](https://doi.org/10.1371/journal.pone.0263026)
- [18] Nikitina M, Kochkina N, Arinina M, et al. Beta-cyclodextrin modified hydrogels of kappa-carrageenan for methotrexate delivery. *Pharmaceutics*. 2023;15(9):2244–2259. doi: [10.3390/pharmaceutics15092244](https://doi.org/10.3390/pharmaceutics15092244)
- [19] Chunshom N, Chuysinuan P, Thanyacharoen T, et al. Development of gallic acid/cyclodextrin inclusion complex in freeze-dried bacterial cellulose and poly (vinyl alcohol) hydrogel: controlled-release characteristic and antioxidant properties. *Mater Chem Phys*. 2019;232:294–300. doi: [10.1016/j.matchemphys.2019.04.070](https://doi.org/10.1016/j.matchemphys.2019.04.070)
- [20] Wu X, Zhang T, Hoff B, et al. Mineralized hydrogels induce bone regeneration in critical size cranial defects. *Adv Healthc Mater*. 2021;10(4):2001101. doi: [10.1002/adhm.202001101](https://doi.org/10.1002/adhm.202001101)
- [21] Aime S, Gianolio E, Palmisano G, et al. Improved syntheses of bis( $\beta$ -cyclodextrin) derivatives, new carriers for gadolinium complexes. *Org Biomol Chem*. 2006;4(6):1124–1130. doi: [10.1039/b517068k](https://doi.org/10.1039/b517068k)
- [22] Kumprecht L, Buděšínský M, Bouř P, et al.  $\alpha$ -cyclodextrins reversibly capped with disulfide bonds. *New J Chem*. 2010;34(10):2254–2260. doi: [10.1039/c0nj00126k](https://doi.org/10.1039/c0nj00126k)
- [23] Jiang Q, Zhang Y, Zhuo R, et al. A light and reduction dual sensitive supramolecular self-assembly gene delivery system based on poly(cyclodextrin) and disulfide-containing azobenzene-terminated branched polyocations. *J Mater Chem B*. 2016;4(47):7731–7740. doi: [10.1039/C6TB02248K](https://doi.org/10.1039/C6TB02248K)



- [24] Gong C, Deng S, Wu Q, et al. Improving antiangiogenesis and anti-tumor activity of curcumin by biodegradable polymeric micelles. *Biomaterials*. 2013;34(4):1413–1432. doi: [10.1016/j.biomaterials.2012.10.068](https://doi.org/10.1016/j.biomaterials.2012.10.068)
- [25] Maheshwari RK, Singh AK, Gaddipati J, et al. Multiple biological activities of curcumin: a short review. *Life Sci*. 2006;78(18):2081–2087. doi: [10.1016/j.lfs.2005.12.007](https://doi.org/10.1016/j.lfs.2005.12.007)
- [26] Duan Y, Cai X, Du H, et al. Novel in situ gel systems based on P123/TPGS mixed micelles and gellan gum for ophthalmic delivery of curcumin. *Colloids Surf B Biointerfaces*. 2015;128:322–330. doi: [10.1016/j.col surfb.2015.02.007](https://doi.org/10.1016/j.col surfb.2015.02.007)
- [27] Mrudula T, Suryanarayana P, Srinivas PN, et al. Effect of curcumin on hyperglycemia-induced vascular endothelial growth factor expression in streptozotocin-induced diabetic rat retina. *Biochem Biophys Res Commun*. 2007;361(2):528–532. doi: [10.1016/j.bbrc.2007.07.059](https://doi.org/10.1016/j.bbrc.2007.07.059)
- [28] Hanif M, Ameer N, Ahmad QU, et al. Improved solubility and corneal permeation of PEGylated curcumin complex used for the treatment of ophthalmic bacterial infections. *PLOS ONE*. 2022;17(4):1–15. doi: [10.1371/journal.pone.0258355](https://doi.org/10.1371/journal.pone.0258355)
- [29] Aboali FA, Habib DA, Elbedaiwy HM, et al. Curcumin-loaded proniosomal gel as a biofriendly alternative for treatment of ocular inflammation: in-vitro and in-vivo assessment. *Int J Pharmaceut*. 2020;589:119835. doi: [10.1016/j.ijpharm.2020.119835](https://doi.org/10.1016/j.ijpharm.2020.119835)
- [30] Cheng Y-H, Fung M-P, Chen Y-Q, et al. Development of mucoadhesive methacrylic anhydride-modified hydroxypropyl methylcellulose hydrogels for topical ocular drug delivery. *J Drug Delivery Sci Technol*. 2024;93:105450. doi: [10.1016/j.jddst.2024.105450](https://doi.org/10.1016/j.jddst.2024.105450)
- [31] Yadav VR, Suresh S, Devi K, et al. Effect of cyclodextrin complexation of curcumin on its solubility and antiangiogenic and anti-inflammatory activity in rat colitis model. *AAPS Pharm Sci Tech*. 2009;10(3):752–762. doi: [10.1208/s12249-009-9264-8](https://doi.org/10.1208/s12249-009-9264-8)
- [32] Liu Y-Y, Fan XD, Gao L. Synthesis and characterization of  $\beta$ -cyclodextrin based functional monomers and its copolymers with N-isopropylacrylamide. *Macromol biosci*. 2003;3(12):715–719. doi: [10.1002/mabi.20030052](https://doi.org/10.1002/mabi.20030052)
- [33] Chen X, Yuk H, Wu J, et al. Instant tough bioadhesive with triggerable benign detachment. *Proc Natl Acad Sci U S A*. 2020;117(27):15497–15503. doi: [10.1073/pnas.2006389117](https://doi.org/10.1073/pnas.2006389117)
- [34] Tranoudis I, Efron N. Water properties of soft contact lens materials. *Contact Lens Anterior Eye*. 2004;27(4):177–191. doi: [10.1016/j.clae.2004.08.002](https://doi.org/10.1016/j.clae.2004.08.002)
- [35] Krystofiak K. Study of dehydration and water states in new and worn soft contact lens materials. *Optica Applicata*. 2014;XLIV(2):237–250.
- [36] Chen F, Le P, Fernandes-Cunha GM, et al. Bio-orthogonally crosslinked hyaluronate-collagen hydrogel for suture-free corneal defect repair. *Biomaterials*. 2020;255:120176. doi: [10.1016/j.biomaterials.2020.120176](https://doi.org/10.1016/j.biomaterials.2020.120176)
- [37] Maulvi FA, Mangukiya MA, Patel PA, et al. Extended release of ketotifen from silica shell nanoparticle-laden hydrogel contact lenses: in vitro and in vivo evaluation. *J Mater Sci Mater Med*. 2016;27(6):113. doi: [10.1007/s10856-016-5724-3](https://doi.org/10.1007/s10856-016-5724-3)
- [38] Jung HJ, Abou-Jaoude M, Carbia BE, et al. Glaucoma therapy by extended release of timolol from nanoparticle loaded silicone-hydrogel contact lenses. *J Control Release*. 2013;165(1):82–89. doi: [10.1016/j.jconrel.2012.10.010](https://doi.org/10.1016/j.jconrel.2012.10.010)
- [39] Hoch G, Chauhan A, Radke CJ. Permeability and diffusivity for water transport through hydrogel membranes. *J Membr Sci*. 2003;214(2):199–209. doi: [10.1016/S0376-7388\(02\)00546-X](https://doi.org/10.1016/S0376-7388(02)00546-X)
- [40] Yang Q, Lai X, Ling J, et al. Facile preparation of hydrogel glue with high strength and antibacterial activity from physically linked network. *Int J Pharm*. 2022;622:121843. doi: [10.1016/j.ijpharm.2022.121843](https://doi.org/10.1016/j.ijpharm.2022.121843)
- [41] Zhao Z, Fan X, Wang S, et al. Natural polymers-enhanced double-network hydrogel as wearable flexible sensor with high mechanical strength and strain sensitivity. *Chin Chem Lett*. 2023;34(6):107892. doi: [10.1016/j.ccllet.2022.107892](https://doi.org/10.1016/j.ccllet.2022.107892)
- [42] Jiang X, Zeng F, Yang X, et al. Injectable self-healing cellulose hydrogel based on host-guest interactions and acylhydrazone bonds for sustained cancer therapy. *Acta Biomater*. 2022;141:102–113. doi: [10.1016/j.actbio.2021.12.036](https://doi.org/10.1016/j.actbio.2021.12.036)
- [43] Jeong D, Joo SW, Shinde VV, et al. Triple-crosslinked beta-cyclodextrin oligomer self-healing hydrogel showing high mechanical strength, enhanced stability and pH responsiveness. *Carbohydr Polym*. 2018;198:563–574. doi: [10.1016/j.carbpol.2018.06.117](https://doi.org/10.1016/j.carbpol.2018.06.117)
- [44] Li R, Guan X, Lin X, et al. Poly(2-hydroxyethyl methacrylate)/beta-cyclodextrin-hyaluronan contact lens with tear protein adsorption resistance and sustained drug delivery for ophthalmic diseases. *Acta Biomater*. 2020;110:105–118. doi: [10.1016/j.actbio.2020.04.002](https://doi.org/10.1016/j.actbio.2020.04.002)
- [45] Xu J, Li X, Sun F. Cyclodextrin-containing hydrogels for contact lenses as a platform for drug incorporation and release. *Acta Biomater*. 2010;6(2):486–493. doi: [10.1016/j.actbio.2009.07.021](https://doi.org/10.1016/j.actbio.2009.07.021)
- [46] Veider F, Haddadzadegan S, Sanchez Armengol E, et al. Inhibition of P-glycoprotein-mediated efflux by thiolated cyclodextrins. *Carbohydr Polym*. 2024;327:121648. doi: [10.1016/j.carbpol.2023.121648](https://doi.org/10.1016/j.carbpol.2023.121648)